



How can urban parks be planned to mitigate urban heat island effect in “Furnace cities”? An accumulation perspective



Xiong Yao ^{a,b,*}, Kunyong Yu ^{b,c}, Xianjun Zeng ^a, Yuebin Lin ^d, Baojian Ye ^a, Xiabing Shen ^a, Jian Liu ^{b,c,**}

^a College of Architecture and Urban Planning, Fujian University of Technology, Fuzhou, 350118, China

^b University Key Lab for Geomatics Technology and Optimize Resources Utilization in Fujian Province, Fuzhou, 350002, China

^c College of Forestry, Fujian Agriculture and Forestry University, Fuzhou, 350002, China

^d College of Design and Innovation, Fujian Jiangxia University, Fuzhou, 350108, China

ARTICLE INFO

Handling Editor: Zhifu Mi

Keywords:

Accumulation-impact cooling index

Cooling island effect

Furnace city

Threshold value of efficiency

Urban green space

Urban planning

ABSTRACT

Urban parks are a major blue-green infrastructure in urban ecosystems, and they are widely regarded as being extremely effective in mitigating the urban heat island (UHI) effect caused by extensive urbanization and high temperatures associated with climate change. A scientific understanding of the cooling effects of urban parks can assist urban planning and decision makers in mitigating the UHI effect and improving urban sustainability. However, little is known about the cooling effects of parks from an accumulation-impact perspective resulting from spatial continuity. In this study, 31 urban parks in Fuzhou, China, were identified using Landsat data, and the land surface temperature was calculated using the radiative transfer equation (RTE) algorithm. Two accumulation-impact cooling indices, the park cooling intensity (PCI) and the park cooling gradient (PCG), and two maximum-impact cooling indices, the park cooling area (PCA) and the park cooling efficiency (PCE), were then used to explore the park cooling effects. The park area and park perimeter were found to be positively and significantly correlated with the PCA, PCI, and PCG and negatively and significantly correlated with the PCE. The results showed that 61% of urban park areas were situated within “cold-spot areas” with respect to the land surface temperature. A ward system cluster analysis showed that the 31 urban parks could be classified into three cooling capacity bundles based on the four normalized park cooling indices, each of which exhibited different cooling effects. The concept of the threshold value of efficiency (TVoE) based on the park cooling gradient was then calculated to determine the optimal park size. The TVoE was determined as 1.08 ha, which implies that urban park planning should consider designing urban parks of this size because they provide the most effective improvement in urban thermal comfort. These findings are valuable for providing a comprehensive understanding of the cooling effects of urban parks and providing implications for sustainable urban planning and design.

1. Introduction

The world is undergoing rapid urbanization; the total urban population has increased from 30% in 1950 to 55% in 2018, and it is expected to reach 68% in 2050 ([United Nations, 2019](#)). This unprecedented process is transforming natural and seminatural land-use types into impervious surfaces and cement-covered areas ([Cetin, 2019](#)). The associated energy balance in the near-surface layer is being significantly

altered, resulting in an urban heat island (UHI) effect, which is a well-known climatic phenomenon characterized by warmer temperatures in urban areas than their surrounding or nearby rural environments ([Ali et al., 2021](#); [Foley et al., 2005](#); [Oke, 1973](#); [Yao et al., 2020](#)). The effects of UHIs may directly or indirectly reduce biodiversity, aggravate heat stress, accelerate energy and water use, and increase air pollution ([Harmay et al., 2021](#)). Thus, such effects threaten the health of urban residents and urban sustainability, particularly during extreme

* Corresponding author. College of Architecture and Urban Planning, Fujian University of Technology, Fuzhou, 350118, China.

** Corresponding author. College of Forestry, Fujian Agriculture and Forestry University, Fuzhou, 350002, China.

E-mail addresses: fjyx@fjut.edu.cn (X. Yao), yuyky@fafu.edu.cn (K. Yu), 39321695@qq.com (X. Zeng), fjlinyuebin@126.com (Y. Lin), yebaojian1989@163.com (B. Ye), sxb@fjut.edu.cn (X. Shen), fjliujian@fafu.edu.cn (J. Liu).

heat events, which is likely to increase mortality (Akbari and Kolokotsa, 2016; Arnfield, 2003; Fouillet et al., 2006; Lin et al., 2017). In addition, there have been significant increases in the frequency and intensity of extreme climate events in the past few decades in the context of global climate change, which has intensified the UHI effect (Montazeri et al., 2017; Yang et al., 2020). In response to these challenges, various urban blue-green infrastructures (such as urban parks, waterbodies, street streets, and green roofs) have been developed to reduce the absorption of solar radiation and the thermal storage capacity, with the aim of mitigating the UHI effect and improving urban comfort (Aram et al., 2019; Fan et al., 2019; Gungor et al., 2021; Manoli et al., 2019; Peng et al., 2020; Sanchez and Reames, 2019; Yang et al., 2017).

Urban parks contribute extensively to the blue and green infrastructure in urban ecosystems (Cetin, 2015); they exert a general cooling effect and can significantly reduce surrounding land surface temperature (LST) (Peng et al., 2021; Yu et al., 2020); for example, LST differences of $>4^{\circ}\text{C}$ were found between urban parks and their surrounding environments in summer (Yang et al., 2017). Therefore, research on the adaptation and mitigation of the UHI effect by urban parks has become a key research focus to improve human welfare and urban sustainability. Numerous studies have been conducted to explore the cooling effects of urban parks by quantifying the park cooling effect, identifying the main impact factors, determining the optimal park size, and planning and designing urban parks (Aram et al., 2019; Cheng et al., 2015; Peng et al., 2021; Yu et al., 2017). To quantify the park cooling effects, many studies have proposed cooling indices, such as the local cool island intensity, which is calculated by subtracting the temperature inside the park from its surrounding temperature (Chang et al., 2007); the cooling effect intensity is calculated by subtracting the LST of the park edges from that inside (Sun et al., 2020). Some studies have introduced cooling indices based on spatial distance, such as the maximum cooling distance, maximum cooling area, and urban cooling island extent (Cheng et al., 2015; Yu et al., 2017). However, although these cooling indices are simple and valuable for exploring the cooling effects of urban parks, they are all calculated based on the maximum-impact perspective. This may lead to unsuitable results when planning and designing an urban park for the following reasons: first, cooling indices based on the maximum-impact perspective cannot comprehensively reflect the spatial variation of LST around urban parks because the cooling effects of parks are spatially continuous and nonlinear (Vidrih and Medved, 2013). Second, the cooling fitting curve (i.e., the relationship between temperature and distance) may change when the maximum cooling indices remain constant, which means that urban parks that have the same maximum cooling distance or area may exert different cooling effects, and these cannot be determined by maximum-impact cooling indices (Peng et al., 2021). Finally, the complex interactions between intrinsic and extrinsic variables involved in the park cooling effect can cause uncertainties in the results. Therefore, to some extent, the use of maximum-impact cooling indices is restrictive when quantifying park cooling effects. To overcome these limitations, in addition to developing maximum-impact cooling indices, it is also necessary to quantify the park cooling effects from the perspective of spatial accumulation. In other words, it is better to explore the park cooling effects based on both maximum-impact and accumulation-impact perspectives when considering adaptation and mitigation of the UHI effect in urban parks.

Previous studies have indicated that it is important for decision makers to determine the threshold size of urban blue-green infrastructures to obtain their optimal cooling efficiencies (Yu et al., 2020). For example, Chang et al. (2007) reported that the threshold size of urban parks in Taipei is 3 ha, and 5.6 ha was determined as the optimal threshold for Leipzig's urban parks and forests (Jaganmohan et al., 2016). From the cost-benefits perspective, Yu et al. (2017) proposed the concept of the threshold value of efficiency (TVoE) to determine the optimal threshold size based on the law of diminishing marginal utility, and this has since been widely used to determine the threshold size of different urban landscapes, such as urban trees, urban

green spaces, and waterbodies (Fan et al., 2019; Peng et al., 2020; Yu et al., 2017). Nevertheless, little is known about the optimal size of urban parks using the TVoE method, and to our knowledge, no studies have explored the threshold size of urban parks from the perspective of TVoE and accumulation impact. It is thus necessary to conduct further studies to fill such research gaps and determine the optimal area of urban parks.

As a new “Furnace city” in China, Fuzhou has experienced severe stress from the UHI effect in the context of urbanization and global climate change (Yu et al., 2018). Urban parks can effectively alleviate the increasingly serious UHI effect and improve the thermal environment. There were 116 documented urban parks in Fuzhou city by the end of 2019, and the green rate in the built-up area reached 42.2%, representing an increase of 0.5% compared to 2018 (Bureau of Statistics, Fuzhou, China). According to the *Urban Overall Planning of Fuzhou city (2011–2020)*, the Fuzhou municipal government plans to build more urban parks in the built-up area to improve urban resilience. Therefore, this study analyzed urban parks in Fuzhou to provide essential information that is currently lacking. The aims of this study were as follows: to (1) quantify the urban parks cooling effects based on the maximum-impact and accumulation-impact perspectives, (2) identify the main factors influencing the park cooling effect, (3) cluster the urban parks based on the maximum-impact and accumulation-impact cooling indices, and (4) quantify the TVoE. The results provide implications for urban park planning and design.

2. Materials and methods

2.1. Study area

The study was conducted in Fuzhou ($118^{\circ}08'\text{E}$ – $120^{\circ}31'\text{E}$, $25^{\circ}15'\text{N}$ – $26^{\circ}39'\text{N}$), which is the capital city of Fujian Province and an important economic center in southeast China (Fig. 1). Fuzhou has a typical subtropical monsoon climate with an average annual frost-free period of over 300 d, an average annual temperature of 19.9°C (Hong et al., 2021), and average annual precipitation of 1502 mm (50% of which occurs from May to August). The average elevation is approximately 84 m above sea level (ranging from 1 m to 802 m) (Hu and Xu, 2018). The Greater Fuzhou metropolitan region includes six urban districts and seven suburban and rural counties, and it covers a total area of approximately $1.2 \times 10^4 \text{ km}^2$. Fuzhou has experienced rapid urbanization in the past two decades, with a permanent population and urbanization rate of 6.38 million and 51.1%, respectively, in 2000 and 8.29 million and 72.5%, respectively, in 2020 (Fuzhou Municipal Statistics Bureau, 2021). Due to rapid urbanization, climate change and improper urban construction activities, Fuzhou has become one of the hottest cities in China since the beginning of the 21st century (Yu et al., 2018). According to the City Temperature List provided by National Climate Center of China in 2013 (<https://www.ncc-cma.net/cn/>), Fuzhou had 37.5 average annual hot days exceeding 35°C during 2000–2009, and it is referred to as a “Furnace city” (Wang and Li, 2014). This study focused on the main urbanized areas of Fuzhou city with a total area of approximately 250 km^2 .

2.2. Data collection and processing

2.2.1. Urban park extraction

An artificial visual interpretation method was used to extract the boundaries of urban parks, and 47 parks were initially extracted using Google Earth as well as a list of parks obtained from the Fuzhou Garden Center. Previous studies have shown that waterbodies connected to parks provide an additional cooling effect (Yu et al., 2017); therefore, urban parks connected to waterbodies were excluded. Thirty-one urban parks, with an average area of 31.16 ha (ranging from 1.30 ha to 321.80 ha), were selected for analysis (Fig. 1). According to the *China Standard for Classification of Urban Green Space* (CJJ/T 85–2017), the 31 urban

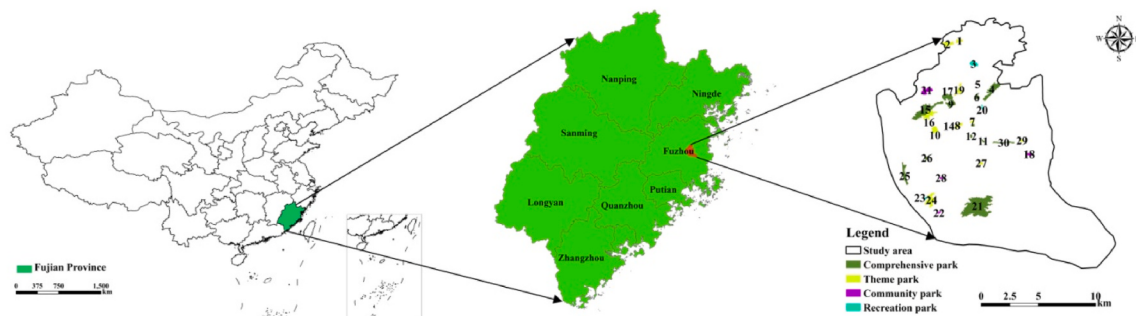


Fig. 1. Location of study area and distribution of 31 urban parks (numbers 1–31).

parks were then classified into four types based on their social use: comprehensive parks (12), theme parks (10), community parks (5), and recreation parks (4).

2.2.2. Land surface temperature retrieval

Previous studies have proven that LST retrieved from remote sensing images can be used to effectively quantify the UHI effect and its relationship with urban landscape patterns (Yao et al., 2020; Yu et al., 2017). Therefore, in this study, Landsat 8 OLI/TIRS images (path 119, row 42) collected on July 27, 2016 from the geospatial data cloud (<http://www.gscloud.cn/>) were used as the original data. The average cloud cover in images was 4.8%; therefore, minimal cloud coverage occurred over the study area, which was beneficial for extracting the urban parks. The images were systematically processed prior to conducting analyses (Hu and Xu, 2018). Although there are two thermal infrared bands (i.e., bands 10 and 11) in Landsat TIRS that can be used to retrieve LST, the calibration parameters in band 11 are unstable. Therefore, the U.S. Geological Survey (USGS) recommends using band 10 to retrieve the LST instead of using a split-window algorithm that uses both bands 10 and 11 (Yu et al., 2017). The study by Jiménez-Muñoz et al. (2009) showed that the single-channel (SC) algorithm is an effective method for use in retrieving LST when the atmospheric water vapor content (W) is $< 3 \text{ g cm}^{-2}$. However, the SC algorithm may not provide accurate results in Fuzhou city because of the high W in summer (Yu et al., 2017). Previous studies have reported that compared to other algorithms, the LST calculated using the radiative transfer equation (RTE) algorithm is the most highly accurate (Yu et al., 2014, 2017), and it was thus adopted in this study to calculate the LST.

The RTE obtains the LST as follows: it mainly uses the atmospheric model to simulate the effect of the atmosphere on surface thermal radiation, and it then subtracts this atmospheric influence part from the total thermal radiation observed by the satellite to obtain the surface thermal radiation intensity, which is then finally converted into the corresponding LST (Jiménez-Muñoz et al., 2014; Yang et al., 2020). In practice, L_λ can be calculated using Eq. (1) (Fan et al., 2019),

$$L_\lambda = [\varepsilon B(T_s) + (1 - \varepsilon)L\downarrow]\tau + L\uparrow \quad (1)$$

where L_λ represents the surface thermal radiation intensity of the thermal infrared band (band 10); ε represents the land surface emissivity calculated based on the normalized difference vegetation index (NDVI) (Zhang et al., 2019); τ , $L\downarrow$, and $L\uparrow$ represent the atmospheric transmissivity, downward radiance, and upward radiance estimated through atmospheric correction, respectively, (<http://atmcorr.gsfc.nasa.gov/>); and $B(T_s)$ and T_s represent the ground radiance and land surface temperature, respectively. According to Plank's law, $B(T_s)$ can be calculated as follows (Yang et al., 2020),

$$B(T_s) = [L_\lambda - L\uparrow - \tau(1 - \varepsilon)L\downarrow] / \tau\varepsilon \quad (2)$$

Finally, the LST can be calculated using the following equation (Fan et al., 2019),

$$T_s = K_2 / \ln(K_1 / B(T_s) + 1) \quad (3)$$

where $K_1 = 774.89 (\text{W m}^{-2} \text{sr}^{-1} \mu\text{m}^{-1})$, and $K_2 = 1321.08 \text{ K}$ (i.e., Kelvin degree) for Landsat 8 TIRS band 10.

2.2.3. Measuring the park cooling effect

It is critical to choose appropriate indicators to measure the park cooling effect. To ensure correspondence with the spatial resolution of the Landsat 8 image (i.e., 30 m), a 300-m wide buffer zone, which was subdivided into ten 30-m wide buffer zones, was established from each urban park boundary to quantify the cooling effect of urban parks. The cubic polynomial function (average $R^2 = 0.9655$ in our study), as shown in Eq. (4), was used to establish the LST-distance relationship for each park (Park et al., 2019),

$$T(l) = al^3 + bl^2 + cl + d \quad (4)$$

where l is the distance between the boundary of the urban park and the buffer zone, and $T(l)$ is the LST at distance l from the boundary of the urban park.

As shown in Fig. 2, the LST in the buffer zone increases with increasing distance from the boundary of the urban park. The maximum LST is reached at a certain point at which the first derivative of the $T(l)$ function ($T'(l)$) is equal to zero; this point is regarded as the first turning point (FTP). The minimum value of the $T'(l)$ function is considered to be the FTP when there is no turning point in the $T(l)$ function. The following is of note: the LST at the FTP is called the surrounding LST (T_D) around the urban park, distance between the boundary of the urban park and the FTP is called the maximum cooling distance (D), and temperature difference between the T_D and mean urban park LST (T_p) is recorded as ΔLST . Therefore, the following four cooling indicators defined by Peng et al. (2021) can be calculated: the park cooling area (PCA), park cooling efficiency (PCE), park cooling intensity (PCI), and park cooling gradient (PCD). Specifically, PCA is defined as the maximum cooling area in which an urban park can cool significantly; PCA has a buffer zone area of width D and can be calculated from the urban park edge; and PCE is the ratio between the PCA and urban park area (S_{park}), and it represents the cooling area per unit urban park area, as shown in Eq. (5),

$$PCE = S_{max} / S_{park} \quad (5)$$

Furthermore, the PCI is the ratio of the reduced LST to the total LST between the urban park boundary and the FTP, and it reflects the cooling sensation felt by local residents. When the PCI is larger, the cooling sensation is more profoundly felt, and it can be calculated using Eq. (6),

$$PCI = \frac{D \times T_D - \int_0^D T(l)dl}{D \times T_D} \quad (6)$$

where D is the maximum cooling distance and T_D is the LST at the maximum cooling distance. Considering that the cooling process is spatially continuous, $D \times T_D$ represents the accumulated temperature of

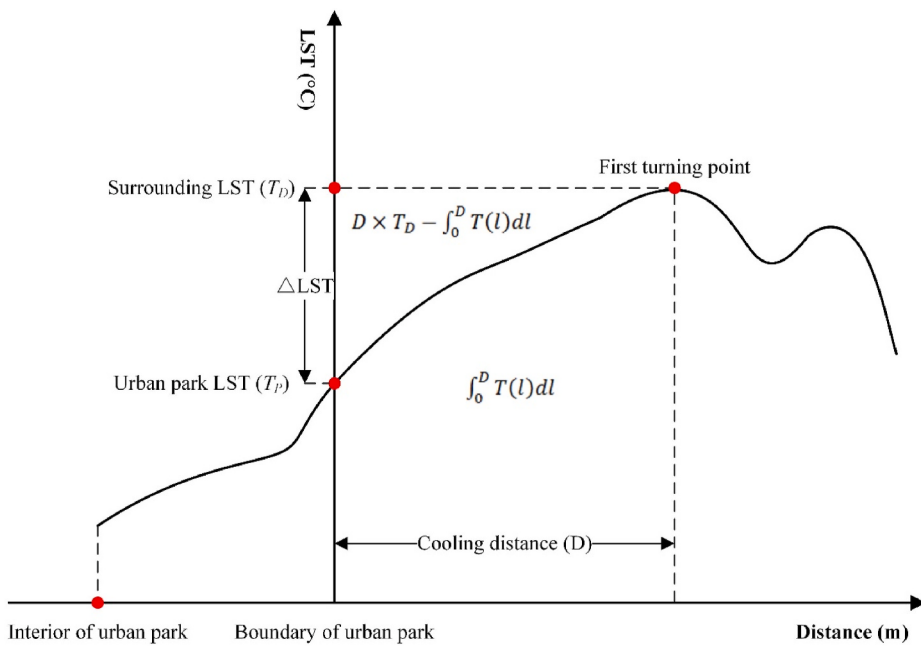


Fig. 2. Schematic of the cooling effect of an urban park.

each continuous point in the absence of an urban park; $\int_0^D T(l)dl$ represents the cumulative sum LSTs at each continuous point from the edge of an urban park; $D \times T_D - \int_0^D T(l)dl$ represents the accumulated temperature difference between urban parks and does not exist. Therefore, the PCI is the ratio of the accumulated temperature reduction (i.e., reduced LST) to the total accumulated temperature (i.e., total LST).

The park cooling gradient (PCG) is the ratio between the reduced LST and the cooling distance, and it indicates the reduction of accumulated temperature per unit park cooling distance (Peng et al., 2021). The PCG reflects the urban park cooling process mode; the larger the PCG, the higher the heat absorption during the cooling process. The PCG is calculated as follows,

$$PCG = \frac{D \times T_D - \int_0^D T(l)dl}{D} \quad (7)$$

2.3. Hot spot analysis (Getis-Ord Gi*)

To interpret the spatial LST heterogeneity, a hot spot analysis (Getis-Ord Gi*) was conducted to analyze spatial cluster arrangements obtained from LST data. This technology can effectively characterize high-value or low-value feature (LST value) clustering areas in the study area. More details regarding hot spot analysis can be found in Tran et al. (2017). Hot spot analysis was performed in ArcGIS 10.2.

2.4. Factors influencing the park cooling effect

Many studies have shown that there is a significant relationship between the size (or shape) of a greenspace and the cooling effect indices. However, the relationship between associated metrics and the park cooling effect has not been adequately clarified, and little attention has been paid to the relationship between landscape patterns and the four park cooling indices (PCA, PCE, PCI, and PCG) (Cheng et al., 2015; Peng et al., 2021; Yu et al., 2018). Therefore, three landscape metrics, namely, the area, perimeter, and landscape shape index (LSI), were used to assist in quantifying the park cooling effect. The LSI calculation is as follows,

$$LSI = \frac{P}{2\sqrt{\pi \times A}} \quad (8)$$

where P and A represent the total perimeter and area of the urban park, respectively. An LSI of 1 and 1.13 indicates that the landscape shape is circular and square, respectively. The greater the LSI, the greater the irregularity of the landscape shape (Sun and Chen, 2012).

Previous studies have shown that the vegetation index (NDVI), which effectively reflects the vegetation biomass status, is positively correlated with the cooling effect of greenspaces (Kuang et al., 2015; Yang et al., 2020). However, the relationship between the modified normalized difference water index (MNDWI), which reflects the area of water bodies inside urban parks, and the park cooling effect remains unclear. Therefore, the NDVI and MNDWI were selected to examine the park cooling effect, and they are calculated as follows,

$$NDVI = \frac{R_{nir} - R_{red}}{R_{nir} + R_{red}} \quad (9)$$

$$MNDWI = \frac{R_{green} - R_{mir}}{R_{green} + R_{mir}} \quad (10)$$

where R_{green} , R_{red} , R_{nir} , and R_{mir} represent the reflection values of the green, red, near-infrared, and middle-infrared bands, which correspond with bands 3, 4, 5, and 6 of the Landsat 8 OLI sensor, respectively.

2.5. Cluster analysis of 31 urban parks

To reduce the influence of the dimensions of the park cooling indices on the clustering results, four park cooling indices were normalized to 0–1 prior to conducting the cluster analysis. A ward system clustering method (also called “the sum of squares of deviation method”) was applied to conduct urban park clustering based on the four normalized park cooling indices. There is no limit to the number of clusters used in the Ward system clustering method; however, in accordance with previous studies, 2–10 clusters were calculated, and the optimal number of clusters was then determined by the minimum number of clusters passing the variance analysis test (Peng et al., 2021). Clustering and variance tests were conducted using SPSS version 21.0 (SPSS Inc., Chicago, IL, USA).

2.6. Determination of threshold value of cooling efficiency (TVoE)

Many studies have reported that nonlinear curves are suitable for fitting the relationship between the cooling effect and influential factors (Peng et al., 2021; Yang et al., 2020). The cooling effect cannot be gradually increased or decreased, and the cooling efficiency is not stable; therefore, it is necessary to determine the TVoE of urban parks. Because the park cooling effect is a nonlinear process and the maximum-impact index (ΔLST) cannot reflect the spatially continuous process of the park cooling effect (Peng et al., 2021), the cumulative index PCG was adopted to determine the TVoE. In practice, a classic parametric logarithmic regression function ($y = \ln x + b$) using a patch size (i.e., the urban park area) as the drive variable was applied to determine the relationship between the PCG and the patch size. As a small-scale park may not produce a positive PCG, the TVoE was considered to be the maximum corresponding park area value of the slope of the resulting logarithmic regression function equaled one (i.e., a) and the PCG equaled zero (i.e., $\text{EXP}(-b/a)$) (Fan et al., 2019; Peng et al., 2020). That is to say, the TVoE was the $\text{EXP}(-b/a)$ when the parameter $\text{EXP}(-b/a)$ was greater than the parameter a (Fig. 3a), and vice versa (Fig. 3b). As shown in Fig. 3b, a small increase in the park area can cause a significant increase in the PCG before the TVoE value; however, the rate of increase continues to decrease with a further increase in the park area. The optimal cooling efficiency is determined when the slope of the fitted curve equals one, based on the principle of using the minimum park area to maximize the PCG. After the TVoE value, there is no significant improvement in the PCG with an increase in the park area. Therefore, the TVoE can be considered the optimal park area in a given city from a cost–benefit perspective (Fan et al., 2019). The TVoE was calculated using OriginPro version 9.0 (OriginLab Corp., Northampton, MA, USA).

2.7. Statistical analysis

The average LST of urban parks and the LST corresponding to the maximum cooling distance was tested for normality using the Shapiro-Wilk test. The above two LST data sets (i.e., average LST of urban parks and T_D) were compared with independent sample t -test. Pearson correlation analysis was used to analyze the relationship between the four cooling indices and the impact factors. All statistical analyses were conducted using SPSS 21.0 (SPSS Inc., Chicago, IL, USA). All significant differences for the statistical analysis were taken at $p < 0.05$ (Yao et al., 2019).

3. Results

3.1. Spatial heterogeneity of LST and its relationship with urban park area

As shown in Fig. 4a, the LST in Fuzhou City ranged from 28.9 °C to 54.5 °C on July 27, 2016 (average 42 °C). There was an obvious spatially heterogeneous LST pattern relationship with landscape type. In detail, the low-LST zone was mainly distributed within blue and green landscape areas, such as urban parks and rivers, whereas the high-LST zone was mainly concentrated within the gray landscape located in densely populated residential and commercial areas. The hot spot analysis results showed that hot and cold regions were related to impervious surfaces and areas with extensive vegetation and river coverage (Fig. 4b), respectively, and these results were consistent with the LST analysis. Moreover, the cold-spot (hot-spot) areas with over 90% confidence overlapped the urban park areas by 61% (0.7%), indicating that urban parks have a significant cooling effect.

The average LST of urban parks ranged from 36.7 °C to 45.5 °C (maximum ΔLST of 8 °C and average LST of 40.6 °C) (Fig. 5a), which was significantly lower ($p < 0.01$) than the T_D and was also lower (by 1.4 °C) than that of Fuzhou city. Again, this result indicates that urban parks significantly mitigate the high LSTs of surrounding areas. In addition, there was a strongly negative logarithmic function relationship between park size and the average LST in urban parks ($R^2 = 0.6634$, $p < 0.001$; Fig. 5b), which suggests the potential effect of park size on the cooling effect.

3.2. Cooling effects of urban parks

The results of calculating the four cooling indicators (the PCA, PCE, PCI, and PCG) are shown in Fig. 6. There were large fluctuations in these four indices between the 31 urban parks. The PCA of parks was within 0.98–184.05 ha (mean 44.19 ha) (Fig. 6a); the PCE of parks was within 0.57–8.43 ha (mean 2.77 ha) (Fig. 6b); the PCI of parks was within 0.0001–0.0479 (mean 0.0181) (Fig. 6c); and the PCG of parks was within 0.01–2.1 °C (mean 0.8 °C) (Fig. 6d). The PCA, PCI, and PCG for most parks showed the same trend, and their lowest and highest values were located in parks 5 and 21 (Fig. 6a, c, and d), respectively. However, there was an opposite trend between the PCA and PCE indices in most parks: the PCA in park 21 was significantly larger than the mean value, whereas the PCE in the same park was the lowest and significantly lower than the mean value (Fig. 6a and b). These differences are primarily attributed to the substantial differences in the sizes of the urban parks (areas ranged from 1.3 ha to 321.8 ha).

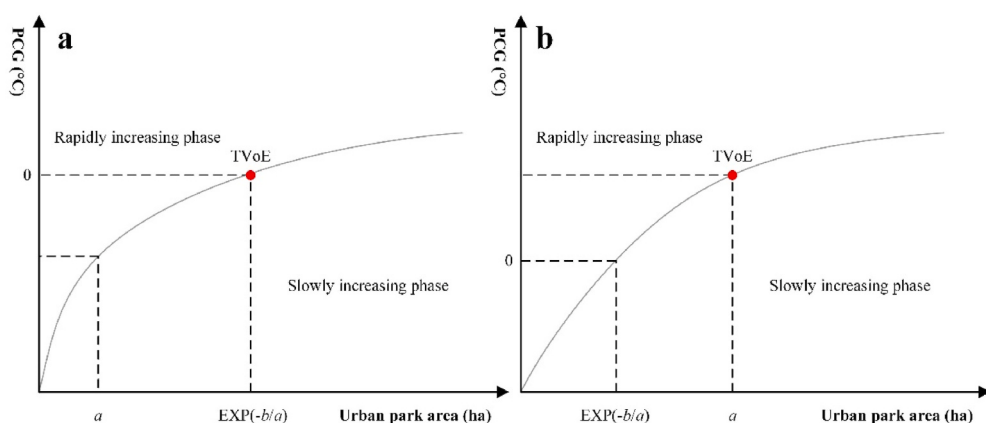


Fig. 3. Schematic of TVoE of urban park.

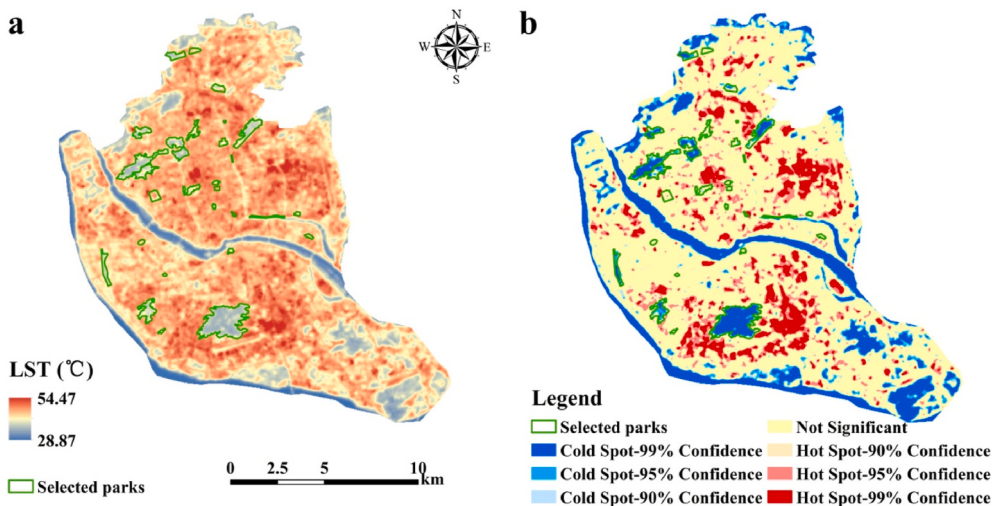


Fig. 4. Spatial distribution of (a) LST and (b) cold-hot spot areas.

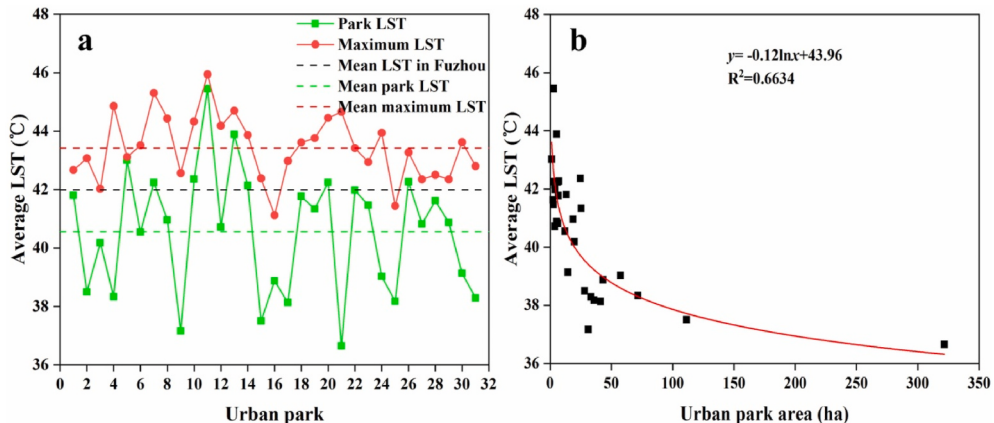


Fig. 5. Urban parks LST and (a) maximum LST, and (b) relationship with park area.

3.3. Relationship between park cooling effects and impact factors

The Pearson correlation coefficients between the four cooling indices (PCA, PCE, PCI, and PCG) and the impact factors (area, perimeter, LSI, NDVI, and MNDWI) were calculated and are shown in Table 1. Many studies have reported that the size of the area and perimeter of parks has a significant influence on the park cooling effect (Brown et al., 2015; Yang et al., 2017). In this study, positive relationships were found between the PCA and the area and perimeter of parks. In addition, the PCA was significantly and positively correlated with the LSI of parks ($r = 0.702$, $p < 0.001$), indicating that urban parks with more complex shapes could effectively create more extensive cooling areas. These results are generally consistent with those reported by Peng et al. (2021).

There was a significant and negative correlation between the PCE and the area and perimeter of parks, which indicates a decrease in the PCE with increasing metrics. However, the reduction in PCE was not significant when the metrics were increased to a certain threshold (Fig. 7a and b). Therefore, it is important to determine this threshold. It was also found that the PCI and PCG were positively correlated with the area and perimeter of parks (Table 1), and a park with a comparatively larger area and perimeter thus has a higher PCI and PCG. Additionally, the NDVI had a significant relationship with the PCA; however, no significant relationship was found with the other cooling indices. Furthermore, no significant correlation was found between the cooling indices and the MNDWI.

3.4. Urban park clustering based on the four cooling indices

The 31 urban parks in our study were divided into three categories based on the clustering and variance test results. According to the definition by Peng et al. (2021), the three categories were referred to as cooling capacity bundles 1, 2, and 3. Subsequently, the park types (comprehensive park, theme park, community park, and recreation park) were compared with the bundles (Table 2). Our results showed that cooling capacity bundle 1 mainly corresponded with theme parks, bundle 2 with comprehensive parks, and bundle 3 with recreation parks.

To analyze the differences between the three cooling capacity bundles, the mean values of the park cooling indices and the impact factors were compared (Fig. 8). The results showed that all four park cooling indices in cooling capacity bundle 1 were low, and the impact factors in these parks were also low. Approximately 50% of the parks in this category were theme parks, with an average area and perimeter of 14.68 ha and 2043.05 m. Cooling capacity bundle 2 related to PCA, PCI, and PCG dominated parks, which indicated large PCA, PCI, and PCG and low PCE values in these parks. Similarly, all mean values of impact factors in these park types were the highest of the three bundles. Most of these park types were comprehensive, with an average area and perimeter of 87.07 ha and 6038.99 m, respectively, which provides a wide and deep cooling effect. Cooling capacity bundle 3 related to PCE-dominated parks. The PCE in this park type was the highest of the four park cooling indices, which indicates a distinctly larger cooling area compared with the park area. Of these park types, 50% were small-scale

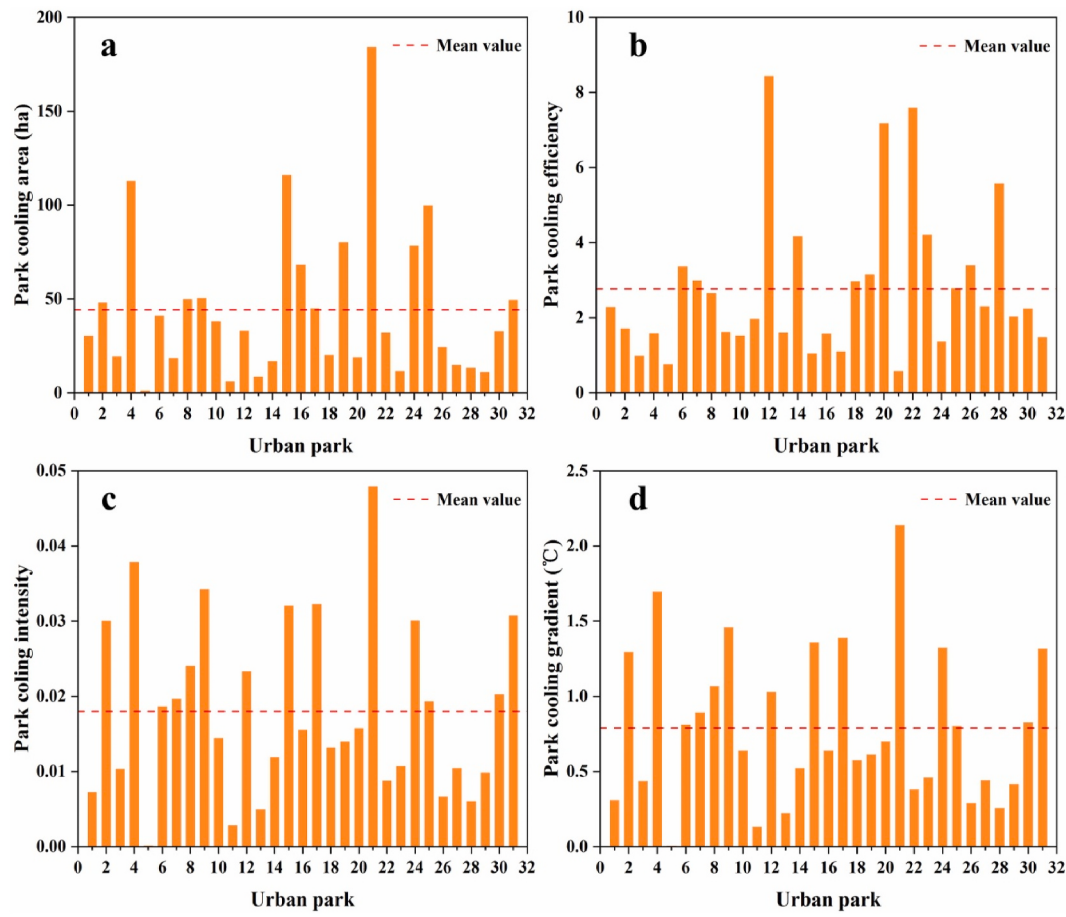


Fig. 6. Four park cooling indices of the 31 urban parks.

Table 1

Correlation coefficients between park cooling effects and impact factors in Fuzhou city.

Cooling indicators	Area	Perimeter	LSI	NDVI	MNDWI
PCA	0.865 ^c	0.954 ^c	0.702 ^c	0.447 ^a	-0.136
PCE	-0.370 ^a	-0.425 ^a	-0.193	-0.035	0.045
PCI	0.692 ^c	0.764 ^c	0.542 ^b	0.327	0.124
PCG	0.701 ^c	0.766 ^c	0.530 ^b	0.329	0.113

^a Significance at the 0.05 level.

^b Significance at the 0.01 level.

^c Significance at the 0.001 level.

Table 2

Urban park types associated with cooling capacity bundle types.

Bundle	Comprehensive park	Theme park	Community park	Recreation park
1	6 (35.29%)	8 (47.06%)	2 (11.76%)	1 (5.88%)
2	5 (62.5%)	2 (25%)	1 (12.5%)	0 (0)
3	1 (16.67%)	0 (0)	2 (33.33%)	3 (50%)

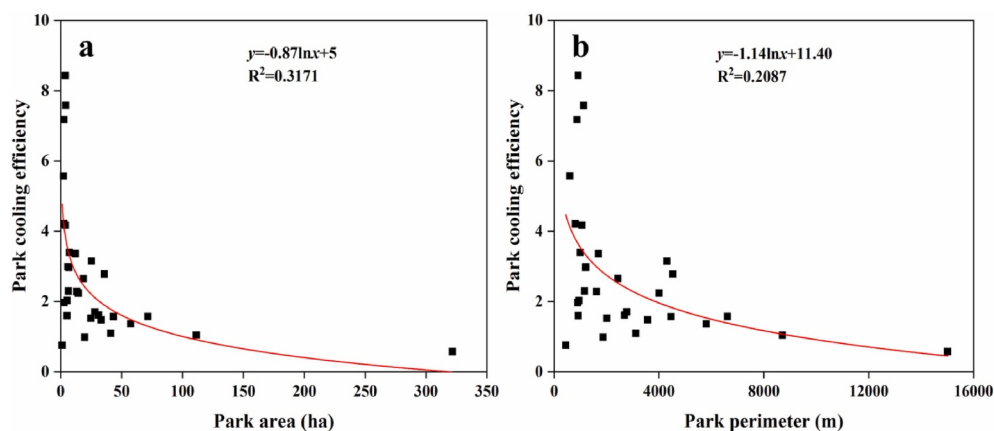


Fig. 7. Relationship between PCE and (a) park area, (b) park perimeter.

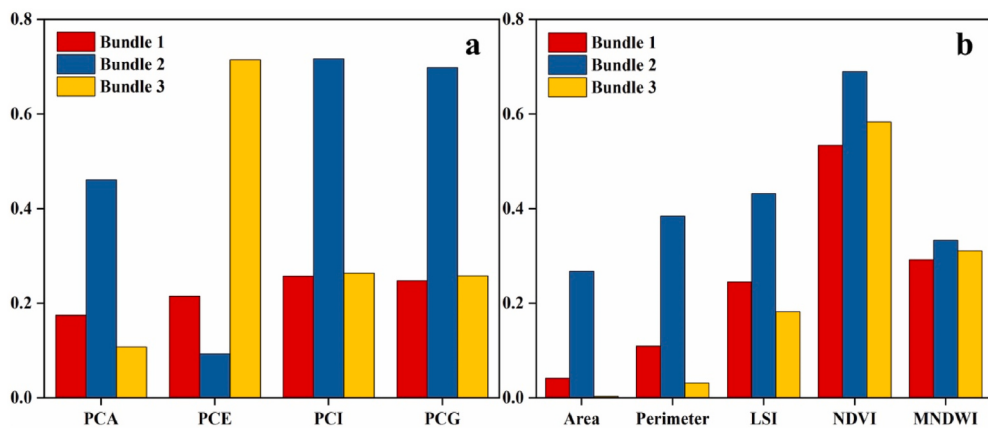


Fig. 8. Histogram of (a) park cooling indices and (b) impact factors in different cooling capacity bundles.

recreation parks with an average area and perimeter of 3.3 ha and 899.84 m. These results show that the classification of urban parks based on the cooling capacity bundles has a strong relationship with the park function, and different park types have differing cooling effects.

3.5. Calculation of TVoE

A logarithmic curve was used to calculate the TVoE of urban parks in Fuzhou City. As shown in Fig. 9, the park area was 0.32 ha when the slope of the resulting logarithmic regression function was one, and the park area was 1.08 ha when the PCG was zero. Thus, the TVoE was determined as 1.08 ha.

4. Discussion

4.1. LST, park cooling effects, and impact factors

Our results indicated that the mean LST in the 31 urban parks was significantly lower than the mean LST of the maximum LST around the urban parks, which shows that the urban parks can effectively mitigate the UHI effect. The largest Δ LST area occurred in Gaogai Mountain park (which has an area greater than 300 ha) on July 27, 2016. However, the Landsat image was collected at 10:32 local time, which was not the warmest part of the day; therefore, the corresponding Δ LST could have been even greater at the hottest time of day (Yang et al., 2017). Our study also found that park area had a significant effect on the LST. Urban parks mainly contain vegetation and waterbodies, which induce cooling,

whereas impervious surfaces account for only a small proportion of the park area; therefore, the larger the area of the urban park, the lower the LST. These findings are in general agreement with those of previous studies (Feyisa et al., 2014; Yang et al., 2017).

In the present study, two accumulation-perspective cooling indices (PCI and PCG) and two maximum-perspective cooling indices (PCA and PCE) were applied to explore the cooling effects of urban parks. Our results showed that the urban parks provided a cooling island effect and, thus an important ecological function. Large differences in park cooling effects were observed between different urban park types; these were related to different factors: intrinsic factors (park area, park perimeter, and waterbody area within park) and extrinsic factors (surrounding land-use type, surrounding building density, and topography) (Hamada et al., 2013; Yang et al., 2017). The park area, park perimeter, and LSI were all significantly and positively correlated with the PCA, PCI, and PCG, and the results followed a similar relationship to those of the intrinsic factors of urban parks and Δ LST (data not shown), which is in agreement with previous studies (Brown et al., 2015; Peng et al., 2021). The MNDWI was not significantly correlated with the park cooling indices. This agrees with the study of Peng et al. (2021); however, other studies have found a significant relationship between MNDWI and cooling indices (Yang et al., 2020). A possible interpretation for this difference is the low proportion of waterbodies in the 31 urban parks (24 urban parks in which less than 10% of the area related to waterbodies). To summarize, park area and park perimeter were found to be the main factors affecting the park cooling effect in this study.

4.2. Implications for urban park planning and design

Several blue-green infrastructure types (urban parks, green roofs (cool roofs), green walls (cool walls), and cool pavements) have been applied to mitigate the UHI effect and to reduce thermal discomfort (Akbari and Kolokotsa, 2016; Imran et al., 2018; Lottrup et al., 2013). In these studies, urban parks have been planned and designed as public spaces that provide multiple purposes; they act as both a leisure space for urban residents while providing a variety of ecosystem services and alleviating the UHI effect (Yu et al., 2017). Some studies have shown that the cooling intensity of a park increases with the size of the park in relation to the enhanced heat exchange between the park and its surrounding environment (Cao et al., 2010; Feyisa et al., 2014). However, although our study verified this effect, the logarithmic relationship found in the present study indicated that PCI does not increase linearly with an increase in the park area. It is not practical to make large increases in the sizes of urban parks (Peng et al., 2020); therefore, it is important to achieve the optimum park cooling effects with the smallest park area when designing urban parks.

Previous studies have considered park cooling effects as part of the

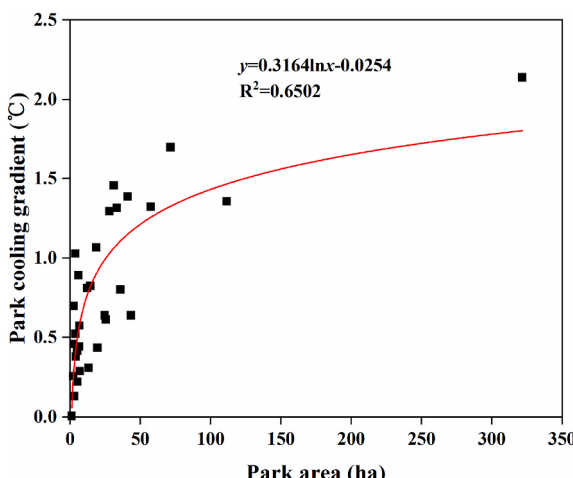


Fig. 9. TVoE of urban park area.

urban park planning and design processes from the maximum-impact perspective. However, such processes have rarely been studied from the accumulation-impact perspective, especially with respect to maximum- and accumulation-impact perspectives (Cheng et al., 2015; Feyisa et al., 2014). Depending on their primary goals and to maximize the benefits of urban parks within the limits of investment, planners and designers need to consider different park cooling effects. In this respect, as the main goal of urban park planning and designing is not to simply optimize a certain cooling index but to improve multiple cooling indices at the same time, it is necessary to consider how to best maximize a certain cooling index without reducing other park cooling indices.

In this study, the TVoE represents the supply and demand relationship of the urban park; a lower TVoE represents higher supply or less demand, and a larger TVoE represents lower supply or higher demand (Peng et al., 2020). The optimum TVoE was found to be 1.08 ha, which is similar to the TVoE of the waterbody in Copenhagen (1.12 ha), but greater than the TVoE of greenspace in Copenhagen (0.69 ha; Yang et al., 2020). This discrepancy may relate to the significantly higher average temperature in Fuzhou ($\sim 35^{\circ}\text{C}$) than in Copenhagen ($\sim 21^{\circ}\text{C}$) during summer. The results obtained here can be used to achieve sustainable urban planning. Urban parks provide different ecosystem service functions, and they need to be planned and designed according to different goals and in consideration of their geographical locations. For example, a small-scale recreation park with a large PCE should be designed when the urban space is limited. If a larger park is required, the PCA, PCI, and PCG will all be large. If an urban park is designed to provide benefits for specific target groups, a community park for community residents or a theme park for children is a good choice. After determining the park type and park size, the landscape pattern and spatial form should be considered to meet the needs of the different urban residents, and urban green landscapes will improve the health and quality of life of residents.

4.3. Study limitations and ideas for future research

This study has certain limitations. First, owing to the restrictions of remote sensing acquisition, the temporal and spatial resolution of Landsat 8 images are limited (spatial resolution of 100 m for TIRS sensor and imaging time at 10:32 in our study). This relatively low resolution and poor imaging time may have increased the uncertainty of the results. Therefore, if remote sensing data acquisition was improved, more LST products with finer resolutions could be used to increase the certainty of results. Second, this study focused on the daytime in a single season (summer) to explore the cooling effects of urban parks. As previous studies have shown, there are seasonal differences in the urban cooling effects and the UHI (Hathway and Sharples, 2012; Peng et al., 2018; Yang et al., 2020). Future studies could be conducted to examine seasonal and diurnal variations in park cooling effects to obtain more accurate results. Third, the influence of waterbodies in urban parks on the park cooling indices requires further study owing to the significant cooling effect of waterbodies on the surrounding LST. Such studies could distinguish the cooling contribution between green and blue landscapes in urban parks and provide further knowledge for use in urban landscape planning and design. To reduce the influence of waterbodies on the additional cooling effects, we excluded urban parks connected with waterbodies in the present study. As a result, the number of selected urban parks (31) was relatively limited, and the results of the cooling capacity bundles and thresholds may have differed if more urban parks had been considered; therefore, applicable conditions for cooling capacity bundles and thresholds could be further explored. Finally, other factors (including socioeconomic development, anthropogenic activities, and building patterns) may affect the park cooling indices (Cetin et al., 2019), and these can also be investigated in subsequent studies.

5. Conclusions

By investigating 31 urban parks in a “Furnace city”, Fuzhou, China, this study used quantitative approaches to analyze the park cooling effects and to determine the optimal park size. The results showed that urban parks provided significant cooling effects; they can cool the surrounding environmental LST by up to 8°C (with an average ΔLST of 2.9°C). The maximum-impact cooling indices and accumulation-impact cooling indices were employed to analyze the park cooling effects, and significant differences in the park cooling effects were found between the urban parks. Urban parks were clustered into three cooling capacity bundles based on the four park cooling indices, and they exhibited different cooling effects. Park area, perimeter, and the LSI were all found to be significantly and positively correlated with the PCA, PCI, and PCG, which means that urban parks with more complex shapes for a given land resource should be planned because of the more cooling areas, cooling intensities, and cooling gradients they create. For urban park size planning, the most efficient size to improve the thermal environment was 1.08 ha, indicating that when the local government implements future urban landscape planning, an urban park size of 1.08 ha was the economically optimal size to mitigate the UHI effect, especially in the context of climate change and the limited land resources. The results of this study enhance our knowledge of the urban park cooling effect and can be used as quantitative guidance for sustainable climate adaptation planning.

CRediT authorship contribution statement

Xiong Yao: Conceptualization, Methodology, Software, Writing – original draft, Funding acquisition. **Kunyong Yu:** Resources, Funding acquisition. **Xianjun Zeng:** Validation, Funding acquisition. **Yuebin Lin:** Formal analysis, Investigation. **Baojian Ye:** Writing – review & editing. **Xiabing Shen:** Writing – review & editing. **Jian Liu:** Writing – review & editing, Supervision.

Declaration of competing interest

The authors declare that they have no known competing financial interests or personal relationships that could have appeared to influence the work reported in this paper.

Acknowledgements

This study was financed by the Natural Science Foundation of Fujian Province, China (grant number 2021J05221); the Education and Research Project for Youth Scholars of Education Department of Fujian Province, China (grant number JAT200353); the National Natural Science Foundation of China (grant numbers 41801160, 41801279, 31770760); the Opening Foundation of State Key Laboratory of Subtropical Building Science (grant number 2020ZB12); and the Scientific Research Foundation of Fujian University of Technology (grant number GY-Z20086).

References

- Akbari, H., Kolokotsa, D., 2016. Three decades of urban heat islands and mitigation technologies research. *Energy Build.* 133, 834–842.
- Ali, G., Abbas, S., Qamer, F.M., Wong, M.S., Rasul, G., Irteza, S.M., Shahzad, N., 2021. Environmental impacts of shifts in energy, emissions, and urban heat island during the COVID-19 lockdown across Pakistan. *J. Clean. Prod.* 291, 125806.
- Aram, F., Solgi, E., Higueras García, E.H., Mosavi, A.R., Várkonyi-Kóczy, A., 2019. The cooling effect of large-scale urban parks on surrounding area thermal comfort. *Energies* 12, 3904.
- Arnfield, A.J., 2003. Two decades of urban climate research: a review of turbulence, exchanges of energy and water, and the urban heat island. *Int. J. Climatol.* 23, 1–26.
- Brown, R.D., Vanos, J., Kenny, N., Lenzholzer, S., 2015. Designing urban parks that ameliorate the effects of climate change. *Lands. Urban Plann.* 138, 118–131.
- Cao, X., Onishi, A., Chen, J., Imura, H., 2010. Quantifying the cool island intensity of urban parks using ASTER and IKONOS data. *Lands. Urban Plann.* 96, 224–231.

- Cetin, M., 2015. Using GIS analysis to assess urban green space in terms of accessibility: case study in Kutahya. *Int. J. Sust. Dev. World.* 22, 420–424.
- Cetin, M., 2019. The effect of urban planning on urban formations determining bioclimatic comfort area's effect using satellite imagines on air quality: a case study of Bursa city. *Air Qual. Atmos. Hlth.* 12, 1237–1249.
- Cetin, M., Adiguzel, F., Gungor, S., Kaya, E., Sancar, M.C., 2019. Evaluation of thermal climatic region areas in terms of building density in urban management and planning for Burdur, Turkey. *Air Qual. Atmos. Hlth.* 12, 1103–1112.
- Chang, C., Li, M., Chang, S., 2007. A preliminary study on the local cool-island intensity of Taipei City parks. *Landscape. Urban Plann.* 80, 386–395.
- Cheng, X., Wei, B., Chen, G., Li, J., Song, C., Urban Plann, J., 2015. Influence of park size and its surrounding urban landscape patterns on the park cooling effect. *Dev.* 141.
- Fan, H., Yu, Z., Yang, G., Liu, T.Y., Liu, T.Y., Hung, C.H., Vejre, H., 2019. How to cool hot-humid (Asian) cities with urban trees? An optimal landscape size perspective. *Agric. For. Meteorol.* 265, 338–348.
- Feyisa, G.L., Dons, K., Meilby, H., 2014. Efficiency of parks in mitigating urban heat island effect: an example from Addis Ababa. *Landscape. Urban Plann.* 123, 87–95.
- Foley, J.A., DeFries, R., Asner, G.P., Barford, C., Bonan, G., Carpenter, S.R., Chapin, F.S., Coe, M.T., Daily, G.C., Gibbs, H.K., Helkowski, J.H., Holloway, T., Howard, E.A., Kucharik, C.J., Monfreda, C., Patz, J.A., Prentice, I.C., Ramankutty, N., Snyder, P.K., 2005. Global consequences of land use. *Science* 309, 570–574.
- Fouillet, A., Rey, G., Laurent, F., Pavillon, G., Bellec, S., Guihenneuc-Jouyaux, C., Clavel, J., Jouglard, E., Hémon, D., 2006. Excess mortality related to the August 2003 heat wave in France. *Int. Arch. Occup. Environ. Health* 80, 16–24.
- Fuzhou Municipal Statistics Bureau, 2021. The seventh national census bulletin of Fuzhou (No. 1) (in Chinese). http://www.fuzhou.gov.cn/tjxx/ndbg/202105/t20210524_4104989.htm.
- Gungor, S., Cetin, M., Adiguzel, F., 2021. Calculation of comfortable thermal conditions for Mersin urban city planning in Turkey. *Air Qual. Atmos. Hlth.* 14, 515–522.
- Hamada, S., Tanaka, T., Ohta, T., 2013. Impacts of land use and topography on the cooling effect of green areas on surrounding urban areas. *Urban For. Urban Green.* 12, 426–434.
- Harmay, N.S.M., Kim, D., Choi, M., 2021. Urban heat island associated with land use/land cover and climate variations in melbourne, Australia. *Sustain. Cities Soc.* 69, 102861.
- Hathway, E.A., Sharples, S., 2012. The interaction of rivers and urban form in mitigating the Urban Heat Island effect: a UK case study. *Build. Environ.* 58, 14–22.
- Hong, X., Wang, G., Liu, J., Song, L., Wu, E.T.Y., 2021. Modeling the impact of soundscape drivers on perceived birdsongs in urban forests. *J. Clean. Prod.* 292, 125315.
- Hu, X., Xu, H., 2018. A new remote sensing index for assessing the spatial heterogeneity in urban ecological quality: a case from Fuzhou City, China. *Ecol. Indicat.* 89, 11–21.
- Imran, H.M., Kala, J., Ng, A.W.M., Muthukumaran, S., 2018. Effectiveness of green and cool roofs in mitigating urban heat island effects during a heatwave event in the city of Melbourne in southeast Australia. *J. Clean. Prod.* 197, 393–405.
- Jaganmohan, M., Knapp, S., Buchmann, C.M., Schwarz, N., 2016. The bigger, the better? The influence of urban green space design on cooling effects for residential areas. *J. Environ. Qual.* 45, 134–145.
- Jiménez-Munoz, J.C., Cristóbal, J., Sobrino, J.A., Soria, G., Ninyerola, M., Pons, X., Pons, X., 2009. Revision of the single-channel algorithm for land surface temperature retrieval from Landsat thermal-infrared data. *IEEE Trans. Geosci. Rem. Sens.* 47, 339–349.
- Jiménez-Munoz, J.C., Sobrino, J.A., Skoković, D., Mattar, C., Cristobal, J., 2014. Land surface temperature retrieval methods from Landsat-8 thermal infrared sensor data. *Geosci. Rem. Sens. Lett. IEEE* 11, 1840–1843.
- Kuang, W., Liu, Y., Dou, Y., Chi, W., Chen, G., Gao, C., Yang, T., Liu, J., Zhang, R., 2015. What are hot and what are not in an urban landscape: quantifying and explaining the land surface temperature pattern in Beijing, China. *Landscape. Ecol.* 30, 357–373.
- Lin, P., Lau, S.S.Y., Qin, H., Gou, Z., 2017. Effects of urban planning indicators on urban heat island: a case study of pocket parks in high-rise high-density environment. *Landscape. Urban Plann.* 168, 48–60.
- Lottrup, L., Grahn, P., Stigsdotter, U.K., 2013. Workplace greenery and perceived level of stress: benefits of access to a green outdoor environment at the workplace. *Landscape. Urban Plann.* 110, 5–11.
- Manoli, G., Fatichi, S., Schläpfer, M., Yu, K., Crwther, T.W., Meili, N., Burland, P., Katul, G.G., Bou-Zeid, E., 2019. Magnitude of urban heat islands largely explained by climate and population. *Nature* 573, 55–60.
- Montazeri, H., Toparlar, Y., Blocken, B., Hensen, J.L.M., 2017. Simulating the cooling effects of water spray systems in urban landscapes: a computational fluid dynamics study in Rotterdam, The Netherlands. *Landscape. Urban Plann.* 159, 85–100.
- Oke, T.R., 1973. City size and the urban heat island. *Atmos. Environ.* 7, 769–779.
- Park, C.Y., Lee, D.K., Asawa, T., Murakami, A., Kim, H.G., Lee, M.K., Lee, H.S., 2019. Influence of urban form on the cooling effect of a small urban river. *Landscape. Urban Plann.* 183, 26–35.
- Peng, J., Dan, Y., Qiao, R., Liu, Y., Dong, J., Wu, J., 2021. How to quantify the cooling effect of urban parks? Linking maximum and accumulation perspectives. *Remote Sens. Environ.* 252, 112135.
- Peng, J., Jia, J., Liu, Y., Li, H., Wu, J., 2018. Seasonal contrast of the dominant factors for spatial distribution of land surface temperature in urban areas. *Remote Sens. Environ.* 215, 255–267.
- Peng, J., Liu, Q., Xu, Z., Lyu, D., Du, Y., Qiao, R., 2020. How to effectively mitigate urban heat island effect? A perspective of waterbody patch size threshold. *Landscape. Urban Plann.* 202, 103873.
- Sanchez, L., Reames, T.G., 2019. Cooling Detroit: a socio-spatial analysis of equity in green roofs as an urban heat island mitigation strategy. *Urban For. Urban Green.* 44, 126331. <http://www.ncbi.nlm.nih.gov/pubmed/126331>.
- Sun, R., Chen, L., 2012. How can urban water bodies be designed for climate adaptation? *Landscape. Urban Plann.* 105, 27–33.
- Sun, X., Tan, X., Chen, K., Song, S., Zhu, X., Hou, D., 2020. Quantifying landscape-metrics impacts on urban green-spaces and water-bodies cooling effect: the study of Nanjing, China. *Urban For. Urban Green.* 55, 126838.
- Tran, D.X., Pla, F., Latorre-Carmona, P., Myint, S.W., Caetano, M., Kieu, H.V., 2017. Characterizing the relationship between land use land cover change and land surface temperature. *ISPRS J. Photogrammetry* 124, 119–132.
- United Nations, Department of Economic and Social Affairs Population Division, 2019. *World Urbanization Prospects: The 2018 Revision (ST/ESA/SER.A/420)*. United Nations, New York.
- Vidrih, B., Medved, S., 2013. Multiparametric model of urban park cooling island. *Urban For. Urban Green.* 12, 220–229.
- Wang, Y., Li, G., 2014. Analysis of "furnace cities" in China using MODIS/LST product (MOD11A2). *Geoscience & Remote Sensing Symposium. IEEE*, pp. 1817–1820.
- Yang, C., He, X., Yu, L., Yang, J., Yan, F., Bu, K., Chang, L., Zhang, S., 2017. The cooling effect of urban parks and its monthly variations in a snow climate city. *Rem. Sens.* 9, 1066.
- Yang, G., Yu, Z., Jørgensen, G., Vejre, H., 2020. How can urban blue-green space be planned for climate adaption in high-latitude cities? A seasonal perspective. *Sustain. Cities Soc.* 53, 101932.
- Yao, L., Li, T., Xu, M., Xu, Y., 2020. How the landscape features of urban green space impact seasonal land surface temperatures at a city-block-scale: an urban heat island study in Beijing, China. *Urban For. Urban Green.* 52, 126704.
- Yao, X., Yu, K., Wang, G., Deng, Y., Lai, Z., Chen, Y., Jiang, Y., Liu, Jian, 2019. Effects of soil erosion and reforestation on soil respiration, organic carbon and nitrogen stocks in an eroded area of Southern China. *Sci. Total Environ.* 683, 98–108.
- Yu, X., Guo, X., Wu, Z., 2014. Land surface temperature retrieval from Landsat 8 TIRS—comparison between radiative transfer equation-based method, split window algorithm and single channel method. *Rem. Sens.* 6, 9829–9852.
- Yu, Z., Guo, X., Jørgensen, G., Vejre, H., 2017. How can urban green spaces be planned for climate adaptation in subtropical cities? *Ecol. Indicat.* 82, 152–162.
- Yu, Z., Guo, X., Zeng, Y., Koga, M., Vejre, H., 2018. Variations in land surface temperature and cooling efficiency of green space in rapid urbanization: the case of Fuzhou city, China. *Urban For. Urban Green.* 29, 113–121.
- Yu, Z., Yang, G., Zuo, S., Jørgensen, G., Koga, M., Vejre, H., 2020. Critical review on the cooling effect of urban blue-green space: a threshold-size perspective. *Urban For. Urban Green.* 49, 126630.
- Zhang, Y., Wang, X., Balzter, H., Qiu, B., Cheng, J., 2019. Directional and zonal analysis of urban thermal environmental change in Fuzhou as an indicator of urban landscape transformation. *Rem. Sens.* 11, 2810.